

Layup Optimization for Buckling of Laminated Composite Shells with Restricted Layer Angles

Cezar Gabriel Diaconu*

University of Bristol, Bristol, England BS8 1TR, United Kingdom

and

Hideki Sekine†

Tohoku University, Sendai 980-8579, Japan

The layup optimization for maximizing buckling loads of long laminated composite cylindrical shells subjected to combinations of axial compression, external lateral pressure, and torsion is carried out on the basis of Flügge's theory. The layer angles, that is, fiber orientation angles, of the laminated composite cylindrical shells are restricted to the values of 0, 45, -45 , and 90 deg, and then nine lamination parameters are used as design variables for the layup optimization. Explicit expressions relating the nine lamination parameters are derived and used to describe the feasible region in the design space of lamination parameters. Thus, the layup optimization problem becomes a constrained nonlinear optimization problem, and the optimum lamination parameters are determined by a mathematical programming method. The laminate configurations aiming to realize the optimum lamination parameters are obtained by analytic formulas or by an unconstrained optimization procedure. It is observed that, for the laminated composite cylindrical shells with the layer angles restricted to the values of 0, 45, -45 , and 90 deg, the optimum buckling loads are less than 10% lower than the optimum buckling loads obtained for unrestricted laminate configurations.

Introduction

THIN-WALLED cylindrical shells subjected to axial compression, lateral pressure, and/or torsion have been widely used for applications in aerospace, naval, automotive, and civil industry. Laminated composites are promising candidates for constructing such structures because they offer higher specific strength and stiffness over traditional materials.

The buckling loads of the laminated composite cylindrical shells are strongly dependent on the laminate configurations and can be maximized by tailoring layer angles, that is, fiber orientation angles, as well as layer thicknesses. Nshanian and Pappas¹ carried out the layup optimization for maximizing buckling loads for various combinations of axial compression and lateral pressure by assuming approximate functions for describing the layer angle distribution through the thickness. For buckling caused by combinations of axial compression, lateral pressure and torsion, the optimum laminate configurations were discussed for laminated composite cylindrical shells with four layers of equal thicknesses.²

In practical applications, layer angles are often restricted to a small set of values such as 0, 45, -45 , and 90 deg. Zimmermann³ proposed design rules to generate a database using these layer angles for a quick optimum design for axial buckling. Also, extensive researches were made to optimize laminated composites with these restricted layer angles and fixed layer thicknesses, using genetic algorithms.^{4–6} Because the genetic algorithms are based on stochastic search, their computational cost is expensive,

and their efficiency is highly dependent on the correct choice of many additional parameters for solving a particular optimization problem.

Instead of layer angles and layer thicknesses, lamination parameters seem to be more reliable design variables because some layup optimization problems become convex and there are no local optima. The in-plane, the coupling, and the out-of-plane stiffnesses can be expressed as linear functions of four in-plane, four coupling, and four out-of-plane lamination parameters. Thus, the mechanical behavior of the laminated composite cylindrical shells related to certain stiffnesses can be optimized using the adequate lamination parameters.

The first attempt for using the 12 lamination parameters in the layup optimization of laminated composite cylindrical shells was conducted in Ref. 7. However, the fundamental properties of lamination parameters were not discussed. Grenestedt and Gudmundson⁸ proved that the 12 lamination parameters are constrained to a convex feasible region. Fukunaga and Vanderplaats⁹ maximized the buckling loads for orthotropic and symmetric laminated composite cylindrical shells subjected to combinations of axial compression and lateral pressure using two in-plane and two out-of-plane lamination parameters as design variables. In the study, the feasible region among these four lamination parameters was provided, though it was proved to be too small by a variational approach.⁸ Using this variational approach, the boundary of the feasible region in the design space of any set of lamination parameters was derived in an implicit manner,¹⁰ and an optimization method, which can use any set of lamination parameters as design variables, was proposed.¹¹ This optimization method was used for maximizing the buckling loads of laminated composite cylindrical shells.¹² Although the optimization method¹¹ gives excellent theoretical results for convex optimization problems, it is rather laborious and unpractical because the explicit expressions relating all 12 of the lamination parameters are unknown.

In the present paper, the layup optimization of long laminated composite cylindrical shells subjected to combinations of axial compression, external lateral pressure, and torsion is carried out on the basis of Flügge's theory. In the buckling analysis of the cylindrical shells, all 12 of the lamination parameters are introduced. The layer angles of the laminated composite cylindrical shells are restricted to the values of 0, 45, -45 , and 90 deg. Thus, three of the lamination

Received 27 February 2003; revision received 15 December 2003; accepted for publication 7 January 2004. Copyright © 2004 by Cezar Gabriel Diaconu and Hideki Sekine. Published by the American Institute of Aeronautics and Astronautics, Inc., with permission. Copies of this paper may be made for personal or internal use, on condition that the copier pay the \$10.00 per-copy fee to the Copyright Clearance Center, Inc., 222 Rosewood Drive, Danvers, MA 01923; include the code 0001-1452/04 \$10.00 in correspondence with the CCC.

*Research Associate, Department of Aerospace Engineering, Queens Building, University Walk; Cz.Diaconu@bristol.ac.uk.

†Professor, Department of Aeronautics and Space Engineering, Aoba-yama 01, Aoba-ku; sekine@plum.mech.tohoku.ac.jp.

parameters vanish, and only nine lamination parameters are necessary for the layout optimization. The explicit expressions describing the feasible region for the nine lamination parameters are derived. The buckling characteristics, that is, buckling loads and buckling modes, are discussed in the design space of the nine lamination parameters. The layout optimization for maximizing the buckling loads of composite laminated cylindrical shells is carried out using a mathematical programming method. The laminate configurations aiming to realize the optimum lamination parameters are also examined.

Buckling Analysis for Laminated Composite Cylindrical Shells

Consider a laminated composite cylindrical shell subjected to combinations loads of axial compression, external lateral pressure, and torsion. The laminated composite cylindrical shell has wall thickness h , length L , and middle surface radius R as shown in Fig. 1. Denoting partial differentiation by a comma, the governing equations for buckling of laminated composite cylindrical shells based on Flügge's theory are expressed in terms of displacements at the middle surface of the shell¹³:

$$H_{11}u + H_{12}v + H_{13}w - N_x^0 u_{,xx} - (N_\phi^0/R)(u_{,\phi\phi}/R - w_{,x}) - 2(N_{x\phi}^0/R)u_{,x\phi} = 0 \quad (1a)$$

$$H_{12}u + H_{22}v + H_{23}w - N_x^0 v_{,xx} - (N_\phi^0/R^2)(w_{,\phi} + v_{,\phi\phi}) - 2(N_{x\phi}^0/R)(w_{,x} + v_{,x\phi}) = 0 \quad (1b)$$

$$H_{13}u + H_{23}v + H_{33}w - N_x^0 w_{,xx} - (N_\phi^0/R)(u_{,x} - v_{,\phi}/R + w_{,\phi\phi}/R) - 2(N_{x\phi}^0/R)(w_{,x\phi} - v_{,x}) = 0 \quad (1c)$$

where u , v , and w denote the displacements at the middle surface in the x , y , and z directions, respectively; N_x^0 , N_ϕ^0 , and $N_{x\phi}^0$ denote the initial stress resultants caused by axial compression, lateral pressure $p = N_\phi^0/R$ and torsion, respectively. The quantities N_x^0 and N_ϕ^0 are positive for axial compression and external lateral pressure, respectively. The differential operators H_{ij} ($i, j = 1, 2, 3$) depend on the stiffnesses of the laminated composite cylindrical shells and are given in the Appendix.

In Eqs. (1), the initial stress resultants can be expressed function of one parameter as

$$N_x^0 = q_x N^0 \quad (2a)$$

$$N_\phi^0 = q_\phi N^0 \quad (2b)$$

$$N_{x\phi}^0 = q_{x\phi} N^0 \quad (2c)$$

where q_x , q_ϕ , and $q_{x\phi}$ are prescribed constants and N^0 is a loading parameter.

For examining the buckling characteristics of laminated composite cylindrical shells, the critical loading parameter N should be

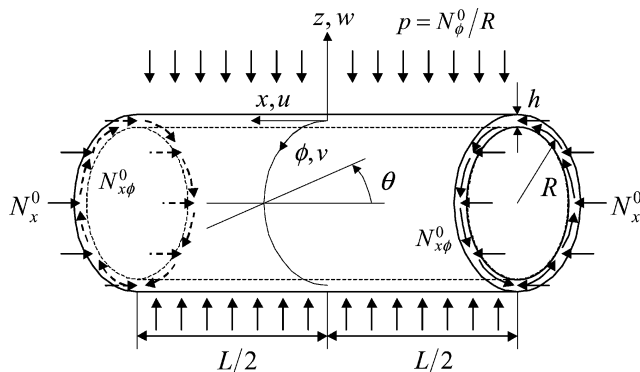


Fig. 1 Laminated composite cylindrical shell.

determined. A solution to Eqs. (1) is given by assuming the following displacements at the middle surface of the cylindrical shells:

$$u = U \sin(\lambda x/R + n\phi) \quad (3a)$$

$$v = V \sin(\lambda x/R + n\phi) \quad (3b)$$

$$w = W \cos(\lambda x/R + n\phi) \quad (3c)$$

where U , V , and W are constants; $\lambda = m\pi R/L$; n is the number of waves in the circumferential direction; and m is the number of half-waves in the axial direction if the circumferential waves do not spin along the cylindrical shells. The displacements in Eqs. (3) cannot satisfy any boundary condition such as simply supported or clamped ends. However, if the cylindrical shell is very long, that is, $L \gg R$, then the constraints at the ends will not affect greatly the magnitude of the buckling loads. Substituting Eqs. (3) into Eqs. (1) and requiring that the determinant of the coefficient matrix vanishes yield a cubic equation in the loading parameter N^0 . From the solutions of the cubic equation solved for a large set of positive integers m and n , the minimum positive loading parameter N^0 gives the critical loading parameter N . Whitney and Sun¹⁴ suggested this reliable method for a quick estimate of the buckling loads.

Laminates with Restricted Layer Angles

Stiffnesses and Lamination Parameters

As given in the Appendix, the differential operators H_{ij} ($i, j = 1, 2, 3$) depend on the stiffnesses A_{ij} , B_{ij} , and D_{ij} ($i, j = 1, 2, 6$) of laminates. Introducing the stiffness invariants and the lamination parameters, the stiffnesses A_{ij} , B_{ij} , and D_{ij} ($i, j = 1, 2, 6$) can be expressed as follows¹⁵:

$$\begin{Bmatrix} A_{11} \\ A_{22} \\ A_{12} \\ A_{66} \\ A_{16} \\ A_{26} \end{Bmatrix} = h \begin{Bmatrix} 1 & \xi_1^A & \xi_2^A & 0 & 0 \\ 1 & -\xi_1^A & \xi_2^A & 0 & 0 \\ 0 & 0 & -\xi_2^A & 1 & 0 \\ 0 & 0 & -\xi_2^A & 0 & 1 \\ 0 & \xi_3^A/2 & \xi_4^A & 0 & 0 \\ 0 & \xi_3^A/2 & -\xi_4^A & 0 & 0 \end{Bmatrix} \begin{Bmatrix} U_1 \\ U_2 \\ U_3 \\ U_4 \\ U_5 \end{Bmatrix} \quad (4a)$$

$$\begin{Bmatrix} B_{11} \\ B_{22} \\ B_{12} \\ B_{66} \\ B_{16} \\ B_{26} \end{Bmatrix} = \frac{h^2}{4} \begin{Bmatrix} 0 & \xi_1^B & \xi_2^B & 0 & 0 \\ 0 & -\xi_1^B & \xi_2^B & 0 & 0 \\ 0 & 0 & -\xi_2^B & 0 & 0 \\ 0 & 0 & -\xi_2^B & 0 & 0 \\ 0 & \xi_3^B/2 & \xi_4^B & 0 & 0 \\ 0 & \xi_3^B/2 & -\xi_4^B & 0 & 0 \end{Bmatrix} \begin{Bmatrix} U_1 \\ U_2 \\ U_3 \\ U_4 \\ U_5 \end{Bmatrix} \quad (4b)$$

$$\begin{Bmatrix} D_{11} \\ D_{22} \\ D_{12} \\ D_{66} \\ D_{16} \\ D_{26} \end{Bmatrix} = \frac{h^3}{12} \begin{Bmatrix} 1 & \xi_1^D & \xi_2^D & 0 & 0 \\ 1 & -\xi_1^D & \xi_2^D & 0 & 0 \\ 0 & 0 & -\xi_2^D & 1 & 0 \\ 0 & 0 & -\xi_2^D & 0 & 1 \\ 0 & \xi_3^D/2 & \xi_4^D & 0 & 0 \\ 0 & \xi_3^D/2 & -\xi_4^D & 0 & 0 \end{Bmatrix} \begin{Bmatrix} U_1 \\ U_2 \\ U_3 \\ U_4 \\ U_5 \end{Bmatrix} \quad (4c)$$

The stiffness invariants U_i ($i = 1, 2, 3, 4, 5$) are material parameters defined next:

$$\begin{Bmatrix} U_1 \\ U_2 \\ U_3 \\ U_4 \\ U_5 \end{Bmatrix} = \begin{Bmatrix} \frac{3}{8} & \frac{3}{8} & \frac{1}{4} & \frac{1}{2} \\ \frac{1}{2} & -\frac{1}{2} & 0 & 0 \\ \frac{1}{8} & \frac{1}{8} & -\frac{1}{4} & -\frac{1}{2} \\ \frac{1}{8} & \frac{1}{8} & \frac{3}{4} & -\frac{1}{2} \\ \frac{1}{8} & \frac{1}{8} & -\frac{1}{4} & \frac{1}{2} \end{Bmatrix} \begin{Bmatrix} Q'_{11} \\ Q'_{22} \\ Q'_{12} \\ Q'_{66} \end{Bmatrix} \quad (5)$$

where

$$Q'_{11} = \frac{E_{11}^2}{(E_{11} - E_{22}v_{12}^2)} \quad (6a)$$

$$Q'_{22} = \frac{E_{11}E_{22}}{(E_{11} - E_{22}v_{12}^2)} \quad (6b)$$

$$Q'_{12} = v_{12}Q'_{22}, \quad Q'_{66} = G_{12} \quad (6c)$$

In Eqs. (6), E_{11} , E_{22} , G_{12} , and v_{12} are engineering constants of a unidirectional lamina. The lamination parameters in Eqs. (4) are defined as follows:

$$\xi_{[1,2,3,4]}^A = \frac{1}{2} \int_{-1}^1 [\cos 2\theta(\bar{z}), \cos 4\theta(\bar{z}), \sin 2\theta(\bar{z}), \sin 4\theta(\bar{z})] d\bar{z} \quad (7a)$$

$$\xi_{[1,2,3,4]}^B = \int_{-1}^1 [\cos 2\theta(\bar{z}), \cos 4\theta(\bar{z}), \sin 2\theta(\bar{z}), \sin 4\theta(\bar{z})] \bar{z} d\bar{z} \quad (7b)$$

$$\xi_{[1,2,3,4]}^D = \frac{3}{2} \int_{-1}^1 [\cos 2\theta(\bar{z}), \cos 4\theta(\bar{z}), \sin 2\theta(\bar{z}), \sin 4\theta(\bar{z})] \bar{z}^2 d\bar{z} \quad (7c)$$

where $\xi_{1,2,3,4}^A$, $\xi_{1,2,3,4}^B$, and $\xi_{1,2,3,4}^D$, respectively, represent the in-plane, the coupling, and the out-of-plane lamination parameters, and $\theta(\bar{z})$ denotes the distribution function of the layer angles through the normalized thickness $\bar{z}(=2z/h)$, which is called henceforth the layup function. Note that the stiffnesses are linear functions of lamination parameters and the critical loading parameter N can be expressed as a function of the 12 lamination parameters when the material properties of lamina and the dimensions of the cylindrical shells are given.

Explicit Expressions Relating Lamination Parameters

In the present approach, the layer angles of the laminated composite cylindrical shells are restricted to the values of 0, 45, -45 , and 90 deg. Thus, $\xi_{1,2,3,4}^{A,B,D} = 0$, and only nine lamination parameters, that is, $\xi_{1,2,3}^A$, $\xi_{1,2,3}^B$, and $\xi_{1,2,3}^D$, are required as design variables for the layup optimization.

For the laminated composite cylindrical shells with layer angles restricted to the values of 0, 45, -45 , and 90 deg, the explicit expressions relating the in-plane and the out-of-plane lamination parameters, that is, $\xi_{1,2,3}^X$ ($X = A, D$), are well known in the literature¹⁶:

$$2|\xi_1^X| - \xi_2^X - 1 \leq 0, \quad X = A, D \quad (8a)$$

$$2|\xi_3^X| + \xi_2^X - 1 \leq 0, \quad X = A, D \quad (8b)$$

The feasible region of $\xi_{1,2,3}^X$ ($X = A, D$) is shown in Fig. 2a. Note that the boundary of the feasible region in the design space of $\xi_{1,2,3}^X$ ($X = A, D$) is made by several plane surfaces.

New explicit expressions relating coupling lamination parameters $\xi_{1,2,3}^B$ can be derived as follows:

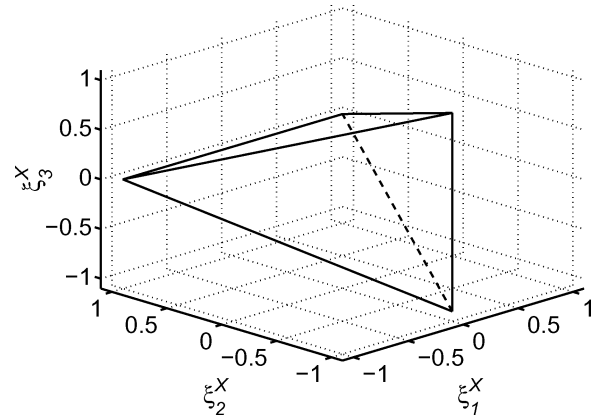
$$2|\xi_1^B| - |\xi_2^B| - 2 \leq 0 \quad (9a)$$

$$2|\xi_3^B| - |\xi_2^B| - 2 \leq 0 \quad (9b)$$

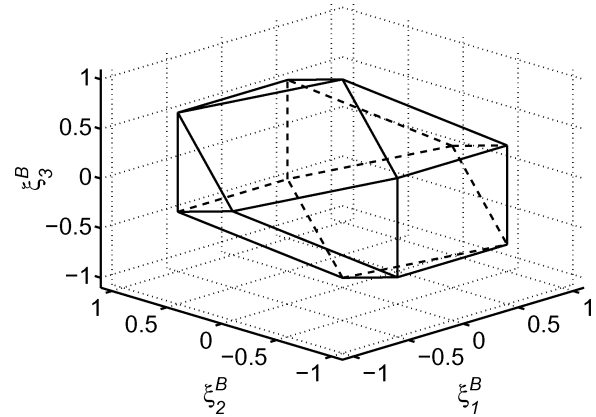
$$|\xi_1^B| + |\xi_3^B| - 1 \leq 0 \quad (9c)$$

The explicit expressions in Eqs. (9) are derived on the basis of a method developed in Ref. 10, as follows. For a given direction $\mathbf{k} = \{k_1^B, k_2^B, k_3^B\}^T$ in the design space of the coupling lamination parameters $\xi_{1,2,3}^B$, the boundary of the feasible region is obtained by determining the layup function $\theta(\bar{z})$, which maximizes the following functional:

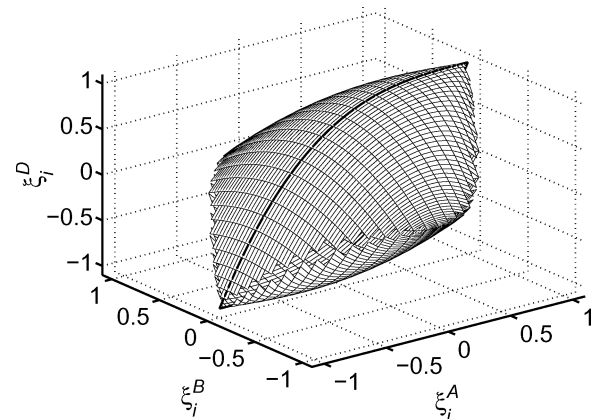
$$F[\theta(\bar{z})] = k_1^B \xi_1^B + k_2^B \xi_2^B + k_3^B \xi_3^B \quad (10)$$



a) $\xi_{1,2,3}^X$ ($X = A, D$)



b) $\xi_{1,2,3}^B$



c) $\xi_i^{A,B,D}$ ($i = 1, 2, 3$)

Fig. 2 Feasible regions.

As an alternative formulation, the following $\Psi(\bar{z})$ should be maximized for determining the layup function $\theta(\bar{z})$ on the boundary of the feasible region:

$$\Psi(\bar{z}) = \begin{cases} \Psi_1(\bar{z}) = 2(2k_2^B + k_1^B)\bar{z} \\ \Psi_2(\bar{z}) = -\Psi_3(\bar{z}) = 2k_3^B\bar{z} \\ \Psi_4(\bar{z}) = 2(2k_2^B - k_1^B)\bar{z} \end{cases} \quad (11)$$

where $\Psi_1(\bar{z})$, $\Psi_2(\bar{z})$, $\Psi_3(\bar{z})$, and $\Psi_4(\bar{z})$ corresponds to the angles 0, 45, -45 , and 90 deg, respectively. Note that the $\Psi_1(\bar{z})$, $\Psi_2(\bar{z})$, $\Psi_3(\bar{z})$, and $\Psi_4(\bar{z})$ are linear functions with respect to \bar{z} , and they intersect in $\bar{z} = 0$. Thus, for most directions \mathbf{k} , there are 12 laminate configurations on the boundary of the feasible region. These 12 laminate configurations are combinations of two layers with equal layer thicknesses and different layer angles and in the design space

of coupling lamination parameters $\xi_{1,2,3}^B$ they are represented as 12 points. By unifying these 12 points, the feasible region is obtained in the forms of Eqs. (9). The feasible region of the design space of coupling lamination parameters $\xi_{1,2,3}^B$ is shown in Fig. 2b. Note that the boundary of the feasible region in the design space of coupling lamination parameters $\xi_{1,2,3}^B$ is also made by several plane surfaces.

Some explicit expressions relating the lamination parameters $\xi_i^{A,B,D}$ ($i = 1, 2, 3$) were previously derived as follows¹²:

$$4(\xi_i^D - 1)(\xi_i^A - 1) \geq (\xi_i^A - 1)^4 + 3(\xi_i^B)^2, \quad i = 1, 2, 3 \quad (12a)$$

$$4(\xi_i^D + 1)(\xi_i^A + 1) \geq (\xi_i^A + 1)^4 + 3(\xi_i^B)^2, \quad i = 1, 2, 3 \quad (12b)$$

The feasible region of $\xi_i^{A,B,D}$ ($i = 1, 2, 3$) is shown in Fig. 2c. In this figure, the thick solid line is given by the explicit expressions derived by Grenestedt and Gudmundson⁸ for the particular case of symmetric and orthotropic laminate configurations.

New explicit expressions relating in-plane, coupling, and out-of-plane lamination parameters can be derived as follows:

$$16(2\xi_1^D - \xi_2^D - 1)(2\xi_1^A - \xi_2^A - 1) \geq (2\xi_1^A - \xi_2^A - 1)^4 + 12(2\xi_1^B - \xi_2^B)^2 \quad (13a)$$

$$16(2\xi_1^D + \xi_2^D + 1)(2\xi_1^A + \xi_2^A + 1) \geq (2\xi_1^A + \xi_2^A + 1)^4 + 12(2\xi_1^B + \xi_2^B)^2 \quad (13b)$$

$$16(2\xi_1^D - \xi_2^D + 3)(2\xi_1^A - \xi_2^A + 3) \geq (2\xi_1^A - \xi_2^A + 3)^4 + 12(2\xi_1^B - \xi_2^B)^2 \quad (13c)$$

$$16(2\xi_1^D + \xi_2^D - 3)(2\xi_1^A + \xi_2^A - 3) \geq (2\xi_1^A + \xi_2^A - 3)^4 + 12(2\xi_1^B + \xi_2^B)^2 \quad (13d)$$

$$16(2\xi_3^D - \xi_2^D + 1)(2\xi_3^A - \xi_2^A + 1) \geq (2\xi_3^A - \xi_2^A + 1)^4 + 12(2\xi_3^B - \xi_2^B)^2 \quad (14a)$$

$$16(2\xi_3^D + \xi_2^D - 1)(2\xi_3^A + \xi_2^A - 1) \geq (2\xi_3^A + \xi_2^A - 1)^4 + 12(2\xi_3^B + \xi_2^B)^2 \quad (14b)$$

$$16(2\xi_3^D - \xi_2^D - 3)(2\xi_3^A - \xi_2^A - 3) \geq (2\xi_3^A - \xi_2^A - 3)^4 + 12(2\xi_3^B - \xi_2^B)^2 \quad (14c)$$

$$16(2\xi_3^D + \xi_2^D + 3)(2\xi_3^A + \xi_2^A + 3) \geq (2\xi_3^A + \xi_2^A + 3)^4 + 12(2\xi_3^B + \xi_2^B)^2 \quad (14d)$$

$$4(\xi_1^D - \xi_3^D - 1)(\xi_1^A - \xi_3^A - 1) \geq (\xi_1^A - \xi_3^A - 1)^4 + 3(\xi_1^B - \xi_3^B)^2 \quad (15a)$$

$$4(\xi_1^D + \xi_3^D + 1)(\xi_1^A + \xi_3^A + 1) \geq (\xi_1^A + \xi_3^A + 1)^4 + 3(\xi_1^B + \xi_3^B)^2 \quad (15b)$$

$$4(\xi_1^D - \xi_3^D + 1)(\xi_1^A - \xi_3^A + 1) \geq (\xi_1^A - \xi_3^A + 1)^4 + 3(\xi_1^B - \xi_3^B)^2 \quad (15c)$$

$$4(\xi_1^D + \xi_3^D - 1)(\xi_1^A + \xi_3^A - 1) \geq (\xi_1^A + \xi_3^A - 1)^4 + 3(\xi_1^B + \xi_3^B)^2 \quad (15d)$$

The explicit expressions in Eqs. (13–15) are derived on the basis of the same method,¹⁰ as follows. For a given direction $\mathbf{k} = \{k_1^A, k_2^A, k_3^A, k_1^B, k_2^B, k_3^B, k_1^D, k_2^D, k_3^D\}^T$ in the design space of the nine lamination parameters $\xi_{1,2,3}^A, \xi_{1,2,3}^B$, and $\xi_{1,2,3}^D$, the boundary of the feasible region is obtained by determining the layup function $\theta(\bar{z})$, which maximizes the following functional:

$$F[\theta(\bar{z})] = k_1^A \xi_1^A + k_2^A \xi_2^A + k_3^A \xi_3^A + k_1^B \xi_1^B + k_2^B \xi_2^B + k_3^B \xi_3^B + k_1^D \xi_1^D + k_2^D \xi_2^D + k_3^D \xi_3^D \quad (16)$$

As an alternative formulation, the following $\Psi(\bar{z})$ should be maximized for determining the layup function $\theta(\bar{z})$ on the boundary of the feasible region:

$$\Psi(\bar{z}) =$$

$$\begin{cases} \Psi_1(\bar{z}) = 3(2k_2^D + k_1^D)\bar{z}^2 + 2(2k_2^B + k_1^B)\bar{z} + (2k_2^A + k_1^A) \\ \Psi_2(\bar{z}) = -\Psi_3(\bar{z}) = 3k_3^D\bar{z}^2 + 2k_3^B\bar{z} + k_3^A \\ \Psi_4(\bar{z}) = 3(2k_2^D - k_1^D)\bar{z}^2 + 2(2k_2^B - k_1^B)\bar{z} + (2k_2^A - k_1^A) \end{cases} \quad (17)$$

where $\Psi_1(\bar{z})$, $\Psi_2(\bar{z})$, $\Psi_3(\bar{z})$, and $\Psi_4(\bar{z})$ correspond to the angles 0, 45, -45, and 90 deg, respectively. Note that in this case $\Psi_1(\bar{z})$, $\Psi_2(\bar{z})$, $\Psi_3(\bar{z})$, and $\Psi_4(\bar{z})$ are parabola and that $\Psi_2(\bar{z}) = -\Psi_3(\bar{z})$. Thus, a maximum number of seven layers describe the layup function on the boundary of the feasible region. Moreover, a maximum number of two layers can have the same layer angle, and the layer angles are symmetric with respect to the middle layer. For example, in case of $\mathbf{k} = \{-0.3, 0.3, 1.0, 0, -0.02, 0.02, 0.25, -0.1, -0.9\}^T$ the laminate configuration $[-45/0/90/45/90/0/-45]$ is obtained as shown in Fig. 3. For this laminate configuration the lamination parameters become

$$\begin{aligned} \xi_1^A &= \frac{1}{2} \left(\int_{-1}^{z_1} 0 d\bar{z} + \int_{z_1}^{z_2} d\bar{z} - \int_{z_2}^{z_3} d\bar{z} \right. \\ &\quad \left. + \int_{z_3}^{z_4} 0 d\bar{z} - \int_{z_4}^{z_5} d\bar{z} + \int_{z_5}^{z_6} d\bar{z} + \int_{z_6}^1 0 d\bar{z} \right) \\ &= \frac{1}{2} (-z_1 + 2z_2 - z_3 + z_4 - 2z_5 + z_6) \end{aligned} \quad (18a)$$

$$\xi_2^A = -1 - z_1 + z_3 - z_4 + z_6 \quad (18b)$$

$$\xi_3^A = -1 + \frac{1}{2} (-z_1 - z_3 + z_4 + z_6) \quad (18c)$$

$$\xi_1^B = -z_1^2 + 2z_2^2 - z_3^2 + z_4^2 - 2z_5^2 + z_6^2 \quad (18d)$$

$$\xi_2^B = -z_1^2 + z_3^2 - z_4^2 + z_6^2 \quad (18e)$$

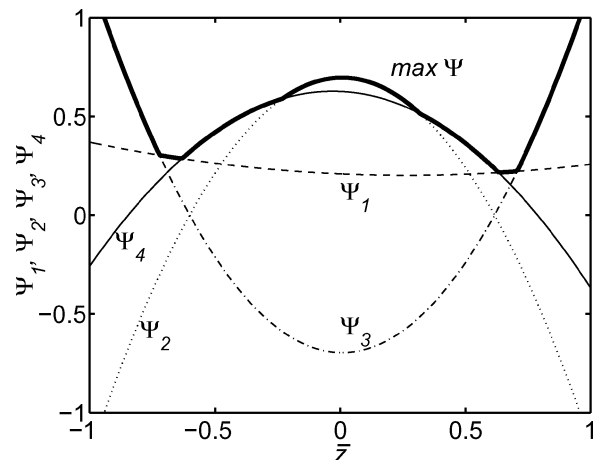


Fig. 3 Laminate configurations on the boundary.

$$\xi_3^B = \frac{1}{2}(-z_1^2 - z_3^2 + z_4^2 + z_6^2) \quad (18f)$$

$$\xi_1^D = \frac{1}{2}(-z_1^3 + 2z_2^3 - z_3^3 + z_4^3 - 2z_5^3 + z_6^3) \quad (18g)$$

$$\xi_2^D = -1 - z_1^3 + z_3^3 - z_4^3 + z_6^3 \quad (18h)$$

$$\xi_3^D = -1 + \frac{1}{2}(-z_1^3 - z_3^3 + z_4^3 + z_6^3) \quad (18i)$$

where z_i ($i = 1, \dots, 6$) are the positions where the layer angles change through the thickness of laminate. From Eqs. (18) the following explicit expressions relating lamination parameters on the boundary of the feasible region are obtained:

$$16(2\xi_3^D - \xi_2^D + 1)(2\xi_3^A - \xi_2^A + 1) = (2\xi_3^A - \xi_2^A + 1)^4 + 12(2\xi_3^B - \xi_2^B)^2 \quad (19a)$$

$$16(2\xi_3^D + \xi_2^D + 3)(2\xi_3^A + \xi_2^A + 3) = (2\xi_3^A + \xi_2^A + 3)^4 + 12(2\xi_3^B + \xi_2^B)^2 \quad (19b)$$

$$4(\xi_1^D - \xi_3^D - 1)(\xi_1^A - \xi_3^A - 1) = (\xi_1^A - \xi_3^A - 1)^4 + 3(\xi_1^B - \xi_3^B)^2 \quad (19c)$$

For lamination parameters inside the feasible region, these expressions become inequalities. There are 24 possible laminate configurations of seven layers with the given restrictions, that is, maximum two layers are allowed to have the same angle and the layer angles are symmetric with respect to the middle layer. By writing the lamination parameters for these laminate configurations, the explicit expressions in Eqs. (12) for $i = 2, (13), (14),$ and (15) are obtained. Note that Eqs. (12) for $i = 1, 3$ are particular cases of Eqs. (13) and (14).

For proving that these explicit expressions completely describe the feasible region in the design space of lamination parameters, an optimization procedure¹¹ was employed. This optimization procedure is carried out to check the feasibility of a given set of lamination parameters ξ_0 . Figure 4 shows the concept of this procedure for a feasible ξ_0 , that is, the feasible region is surrounded by the solid line. In the design space of the lamination parameters, we can obtain a hyperplane $F = k^T \xi$ normal to a given direction k and tangent to the feasible region.¹⁰ The hyperplane F intersects ξ_0 at the point ξ_Q . Thus, the feasibility of ξ_0 can be determined by minimizing the norm D of ξ_Q taking the components of k as design variables. The initial set of design variables is chosen such that k makes an acute angle with ξ_0 , that is, $k^T \xi_0 > 0$. The norm D is defined as follows:

$$D = \|k^T \xi / k^T \xi_0\| \quad (20)$$

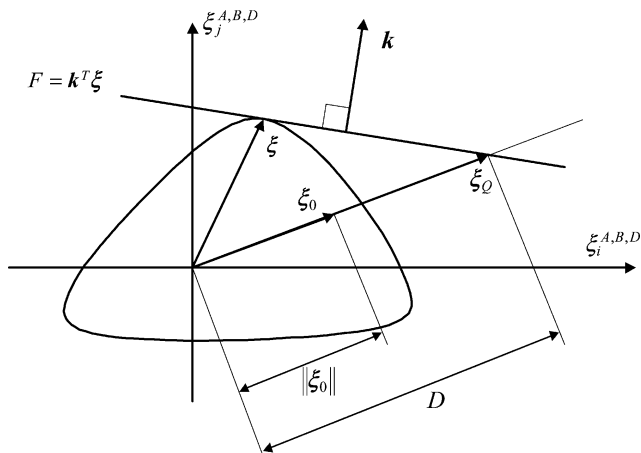


Fig. 4 Optimization procedure for verifying the explicit expressions.

where

$$\bar{\xi}_0 = \xi_0 / \|\xi_0\| \quad (21)$$

Thus, this optimization procedure is stated as follows.

Minimize:

$$D(k)$$

Design variables:

$$k = \{k_1^A, k_2^A, k_3^A, k_1^B, k_2^B, k_3^B, k_1^D, k_2^D, k_3^D\}^T$$

The output of this procedure is the optimum $\xi_Q (= \min D \bar{\xi}_0)$ on the boundary of the feasible region, and the condition for a feasible ξ_0 is $\min D \geq \|\xi_0\|$. For all of the randomly generated lamination parameters fulfilling the explicit expressions in Eqs. (8), (9), (12–15), this condition was not violated. Moreover, the lamination parameters that lie on the boundary of the region described by the explicit expressions also lie on the boundary of the feasible region, that is, $\min D = \|\xi_0\|$. This proves that the explicit expressions in Eqs. (8), (9), and (12–15) are sufficient to describe the feasible region in the design space of the nine lamination parameters $\xi_{1,2,3}^A, \xi_{1,2,3}^B$, and $\xi_{1,2,3}^D$ when the layer angles of the laminated composite cylindrical shells are restricted to the values of 0, 45, –45, and 90 deg. (Note that, in the present approach, a large region of the design space of lamination parameters remain unused because $\xi_4^{A,B,D} = 0$. For using this region, that is, for having $\xi_4^{A,B,D} \neq 0$, other layer angles such as ± 22.5 and ± 67.5 deg, should be also allowed in the laminate configurations.)

Laminate Configurations for Given Lamination Parameters

This subsection treats the inverse problem of finding the laminate configuration for a given set of feasible lamination parameters. For the particular cases of cross-ply laminate configurations, that is, the layer angles are restricted to $\theta_1 = 0$ and $\theta_2 = 90$ deg, and angle-ply laminate configurations, that is, the layer angles are restricted to $\theta_1 = 45$ and $\theta_2 = -45$ deg, only three lamination parameters, $\xi_1^{A,B,D}$ and $\xi_3^{A,B,D}$, respectively, are variable, whereas the others are fixed as shown in Table 1. For these two cases the laminate configurations can be easily determined by calculating the positions z_j ($j = 1, 2, 3$), where the layer angles θ_1 and θ_2 change through the thickness, using the formulas given in Table 2. These formulas were obtained for the lamination parameters $\xi_i^{A,B,D}$ ($i = 1, 3$) in the same manner¹² used to derive the explicit expressions in Eqs. (12). Table 2 gives the formulas for symmetric and nonsymmetric laminate configurations when the lamination parameters $\xi_i^{A,B,D}$ ($i = 1, 3$) are on the boundary or inside the feasible region given by Eqs. (12) for $i = 1, 3$. For lamination parameters lying on the boundary of the feasible region, a unique laminate configuration can be determined using the formulas given in Table 2. However, for the lamination parameters inside the feasible region, the laminate configuration is not unique, and two different laminate configurations can be determined using the formulas given in Table 2. Note that Eqs. (12) for $i = 1, 3$ are sufficient to describe the feasible region for cross-ply laminate configurations, that is, explicit expressions relating $\xi_1^{A,B,D}$, and for angle-ply laminate configurations, that is, explicit expressions relating $\xi_3^{A,B,D}$. Also, only four layers are sufficient to describe the feasible region.

For the general case of laminates with layer angles restricted to the values of 0, 45, –45, and 90 deg, an optimization procedure is employed in order to determine a laminate configuration aiming to

Table 1 Lamination parameters for fixed layer angles

Laminate type	Layer angles		Lamination parameters	
	θ_1	θ_2	Fixed	Variable
Cross ply	0	90	$\xi_{3,4}^{A,D} = \xi_{2,3,4}^B = 0, \xi_2^{A,D} = 1$	$\xi_1^{A,B,D}$
Angle ply	45	–45	$\xi_{1,4}^{A,D} = \xi_{1,2,4}^B = 0, \xi_2^{A,D} = -1$	$\xi_3^{A,B,D}$

Table 2 Laminate configurations for lamination parameters $\xi_i^{A,B,D}$ ($i = 1, 3$)

Position	Laminate configuration	Top of laminae z_j ($j = 1, 2, 3$)	Notation
On boundary	$\left[(\theta_1)_{1-z_1} / (\theta_2)_{z_1} \right]_S$	$z_1 = -a$	$a = (\xi_i^A - 1) / 2$
	$\left[(\theta_2)_{1-z_1} / (\theta_1)_{z_1} \right]_S$	$z_1 = a$	$a = (\xi_i^A + 1) / 2$
Inside	$\left[(\theta_1)_{1-z_2} / (\theta_2)_{z_2-z_1} / (\theta_1)_{z_1} \right]_S$	$z_{1,2} = [\pm 3a^2 - \sqrt{3a(4d - a^3)}] / 6a$	$a = (\xi_i^A - 1) / 2$ $d = (\xi_i^D - 1) / 2$
	$\left[(\theta_2)_{1-z_2} / (\theta_1)_{z_2-z_1} / (\theta_2)_{z_1} \right]_S$	$z_{1,2} = [\mp 3a^2 + \sqrt{3a(4d - a^3)}] / 6a$	$a = (\xi_i^A + 1) / 2$ $d = (\xi_i^D + 1) / 2$
On boundary	$\left[(\theta_1)_{z_1+1} / (\theta_2)_{z_2-z_1} / (\theta_1)_{1-z_2} \right]$	$z_1 = (b + a^2) / 2a, z_2 = (b - a^2) / 2a$	$a = \xi_i^A - 1$ $b = \xi_i^B$
	$\left[(\theta_2)_{z_1+1} / (\theta_1)_{z_2-z_1} / (\theta_2)_{1-z_2} \right]$	$z_1 = (b - a^2) / 2a, z_2 = (b + a^2) / 2a$	$a = \xi_i^A + 1$ $b = \xi_i^B$
Inside	$\left[(\theta_1)_{z_1+1} / (\theta_2)_{z_2-z_1} / (\theta_1)_{z_3-z_2} / (\theta_2)_{1-z_3} \right]$	$z_{1,3} = [2(d - a^3) \pm \sqrt{4d^2 + 16a^3d - 2a^6 - 24abd + 6a^4b + 18b^3 - 18a^2b^2}] / 6(b - a^2)$	$a = \xi_i^A$ $b = \xi_i^B + 1$ $d = \xi_i^D$
	$\left[(\theta_2)_{z_1+1} / (\theta_1)_{z_2-z_1} / (\theta_2)_{z_3-z_2} / (\theta_1)_{1-z_3} \right]$	$z_2 = (b - a^2) / 2(a - z_{1,3}) + z_{1,3}$	$a = -\xi_i^A$ $b = 1 - \xi_i^B$ $d = -\xi_i^D$

realize a set of feasible lamination parameters ξ_0 . The design variables are the layer thicknesses of 12-layered laminates and the layer angles fixed and ordered as $[-45/0/45/90/\dots/-45/0/45/90]$. We consider that such a laminate configuration is sufficient to cover all possible laminate configurations corresponding to lamination parameters on the boundary and inside the feasible region. The objective function is defined by

$$\Delta\xi = \sum_{i=1}^3 w_i^A (\xi_{i0}^A - \tilde{\xi}_i^A)^2 + \sum_{i=1}^3 w_i^B (\xi_{i0}^B - \tilde{\xi}_i^B)^2 + \sum_{i=1}^3 w_i^D (\xi_{i0}^D - \tilde{\xi}_i^D)^2 \quad (22)$$

where $\tilde{\xi}_{1,2,3}^A$, $\tilde{\xi}_{1,2,3}^B$, and $\tilde{\xi}_{1,2,3}^D$ denote the lamination parameters calculated from the laminate configurations and $w_{1,2,3}^A$, $w_{1,2,3}^B$, and $w_{1,2,3}^D$ denote weighting functions. Thus, the optimization problem for determining the laminate configuration aiming to realize a given set of lamination parameters is stated as follows.

Minimize:

$$\Delta\xi(\mathbf{h})$$

Design variables:

$$\mathbf{h} = \{h_1, h_2, \dots, h_{12}\}^T$$

When the condition $\Delta\xi \leq \varepsilon$ is satisfied for a small value of ε , we obtain one laminate configuration corresponding to ξ_0 . At least one laminate configuration exists for a set of feasible lamination parameters ξ_0 . When nonunique laminate configurations exist for ξ_0 , this optimization procedure can provide several examples of laminate configurations depending on the choice of the initial design variables.

Note that, for certain cases when lamination parameters are at the corners of the feasible regions in Fig. 2, the laminate configurations, provided by the formulas given in Table 2 or by the optimization procedure just employed, are unidirectional single layers or combinations of two layers with equal layer thicknesses. For all of the other situations, the formulas given in Table 2 as well as the optimization procedure just employed can give only laminate configurations without a physical meaning because the layer thicknesses are not integer. However, in practice, laminate configurations with integer layer thicknesses can be obtained by minimizing the objective function given in Eq. (22) using discrete optimization methods.

For most practical situations, the laminate configurations will be obtained using discrete optimization methods and the set of lamination parameters ξ calculated from these laminate configurations will not be identical with the set of feasible lamination parameters ξ_0 . In this case, the best laminate configuration can be selected among alternate possible designs by a proper choice of the weighting functions $w_{1,2,3}^X$ ($X = A, B, D$).

Buckling Characteristics

In this section, the buckling characteristics, that is, buckling loads and buckling modes, of long laminated composite cylindrical shells subjected to combinations of axial compression, lateral pressure, and torsion are discussed in the design space of lamination parameters. As a numerical example, we consider laminated graphite/epoxy cylindrical shells that are assumed perfect, free of eccentricity, and other manufacture imperfections. The material properties of the lamina are given here: $E_{11}/E_{22} = 20$; $G_{12}/E_{22} = 0.6$; and $\nu_{12} = 0.25$. The cylindrical shells have the length-to-radius ratio of $L/R = 125$ and the radius-to-thickness ratio of $R/h = 20$. The critical loading parameter is normalized as follows:

$$\bar{N} = N/E_{22}h \times 10^3 \quad (23)$$

Thus, the normalized buckling loads of the laminated composite cylindrical shells subjected to axial compression, lateral pressure, and torsion are

$$\bar{N}_x = q_x \bar{N} \quad (24a)$$

$$\bar{N}_\phi = q_\phi \bar{N} \quad (24b)$$

$$\bar{N}_{x\phi} = q_{x\phi} \bar{N} \quad (24c)$$

Figures 5–7 show the buckling characteristics of long laminated composite cylindrical shells for axial compression, lateral pressure, and torsion, respectively. In each figure the contours of the normalized loading parameter \bar{N} are plotted on ξ_i^A, ξ_i^D ($i = 1, 2, 3$) planes: a) ξ_1^A, ξ_1^D plane for $\xi_{3,4}^{A,D} = \xi_{1,2,3,4}^B = 0, \xi_2^{A,D} = 1$; b) ξ_2^A, ξ_2^D plane for $\xi_{1,3,4}^{A,D} = \xi_{1,2,3,4}^B = 0$; and c) ξ_3^A, ξ_3^D plane for $\xi_{1,4}^{A,D} = \xi_{1,2,3,4}^B = 0, \xi_2^{A,D} = -1$. The contours are shown inside the feasible region depicted by a solid line. Cases a and c correspond to symmetric cross-ply laminate configurations and symmetric angle-ply laminate configurations, respectively. Case b corresponds to symmetric laminate configurations with infinitesimal layer thicknesses and balanced layer angles of 0, 45, -45 , and 90 deg. Although cases a and

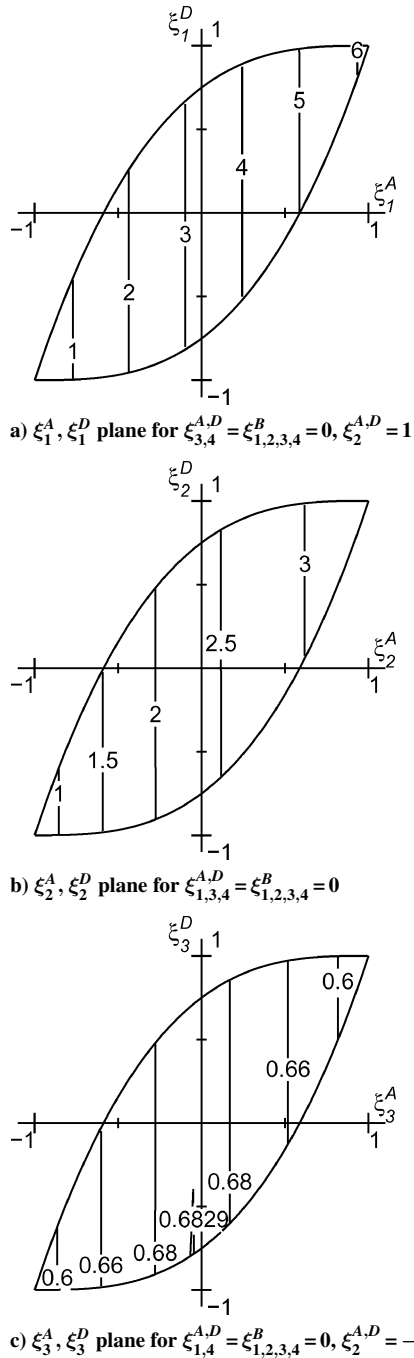


Fig. 5 Contours of \bar{N} for axial compression, that is, $q_x = 1, q_\phi = q_{x\phi} = 0$.

c correspond to practical situations, case b has no practical meaning. Case b is used to make the connection between the cross-ply laminate configurations and the angle-ply laminate configurations.

Figure 5 shows the contours of \bar{N} for the case of axial compression, that is, $q_x = 1, q_\phi = q_{x\phi} = 0$. Euler buckling mode, that is, $m = n = 1$, occurs when the cylindrical shells buckle. The contours of \bar{N} are almost vertical lines, which means that the in-plane lamination parameters $\xi_{1,2,3}^A$ have the main influence for Euler buckling under axial compression. Moreover, the maximum \bar{N} can be observed in Fig. 5a for $\xi_1^A = \xi_1^D = 1$, that is, single-layer laminate configuration [0].

Figure 6 shows the contours of \bar{N} for the case of lateral pressure, that is, $q_\phi = 1, q_x = q_{x\phi} = 0$. For this case local buckling mode, that is, $m \neq 1$ and $n \neq 1$, occurs when the cylindrical shells buckle. In this case the contours of \bar{N} are horizontal lines, which means that the out-of-plane lamination parameters $\xi_{1,2,3}^D$ have the main influence for buckling under lateral pressure, and the maximum \bar{N} can be

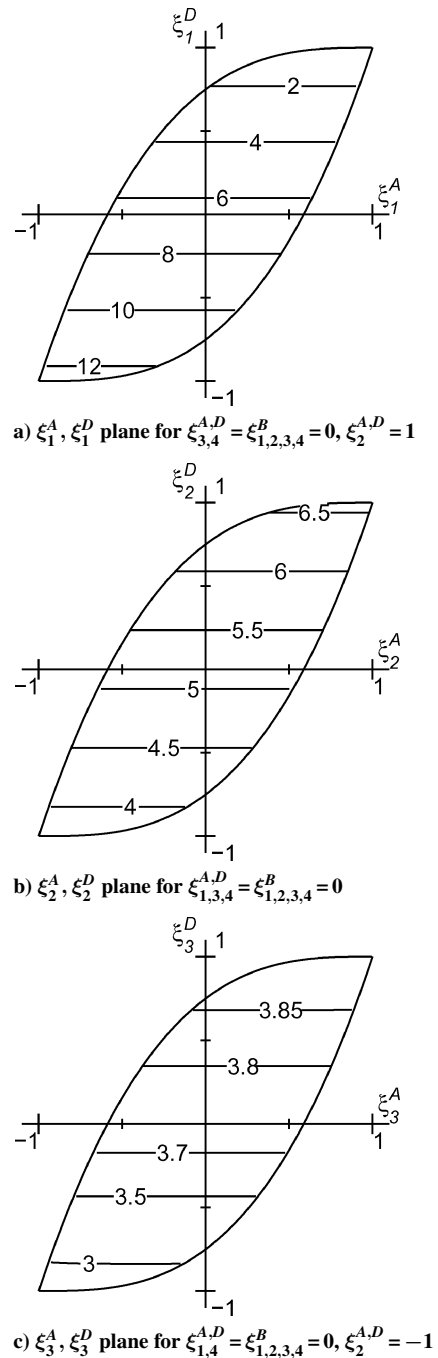


Fig. 6 Contours of \bar{N} for lateral pressure, that is, $q_\phi = 1, q_x = q_{x\phi} = 0$.

observed in Fig. 6a for $\xi_1^A = \xi_1^D = -1$, that is, single-layer laminate configuration [90].

Figure 7 shows the contours of \bar{N} for the case of torsion, that is, $q_{x\phi} = 1, q_x = q_\phi = 0$. For this case, both Euler and local buckling modes occur when the cylindrical shells buckle. However, Euler buckling mode can be observed only in the left down corner of ξ_1^A, ξ_1^D plane in Fig. 7a as shown by the contours of \bar{N} represented as vertical lines. All of the other regions of the lamination parameters planes are covered by local buckling modes depicted by the curved contours of \bar{N} . The maximum \bar{N} can be observed in Fig. 7a at the lower boundary of the feasible region, which corresponds to a $[90/0]_S$ laminate configuration.

Figure 8 shows the contours of \bar{N} for combined loads, that is, $q_x = 0.1, q_\phi = 0.05$, and $q_{x\phi} = 1$ in the design space of lamination parameters for cross-ply laminate configurations. In Fig. 8 both Euler and local buckling modes occur. However, Euler buckling mode can be observed only on ξ_1^A, ξ_1^D and ξ_1^A, ξ_1^B planes in Figs. 8a

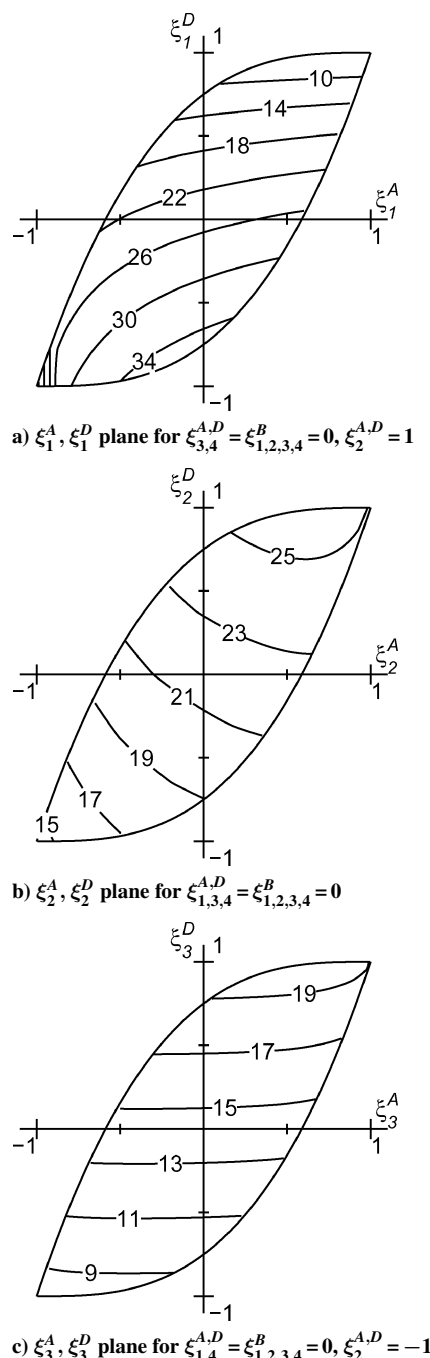


Fig. 7 Contours of \bar{N} for torsion, that is, $q_{x\phi} = 1, q_x = q_\phi = 0$.

and 8b as shown by the contours of \bar{N} represented as vertical lines. Note that in Figs. 8b and 8c the contours of \bar{N} in ξ_1^A, ξ_1^B plane and ξ_1^B, ξ_1^D plane are almost symmetric with respect to ξ_1^A and ξ_1^D axes, respectively. Moreover, from Figs. 8a and 8c it can be observed that the maximum \bar{N} lies on the lower boundary of the feasible region at $\xi_1^B \simeq 0$, which corresponds to an almost symmetric laminate configuration [90/0/90].

Layup Optimization

To find the laminate configurations that maximize the buckling loads of the long laminated cylindrical shells, the nine lamination parameters $\xi_{1,2,3}^A, \xi_{1,2,3}^B$, and $\xi_{1,2,3}^D$ are used as design variables, and $\xi_4^{A,B,D} = 0$ are imposed. The layup optimization problem is stated as follows.

Maximize:

$$\bar{N}(\xi)$$

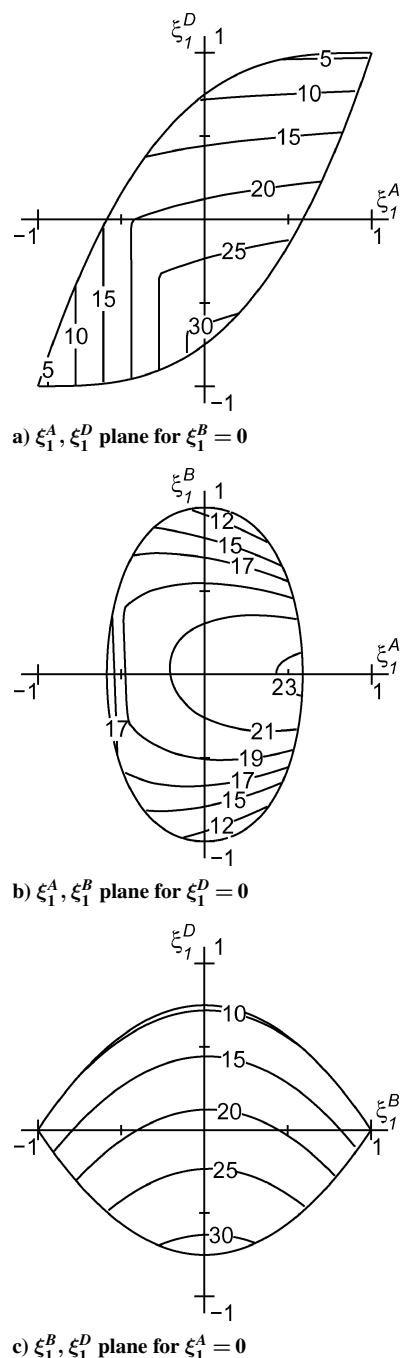


Fig. 8 Contours of \bar{N} for combined loads, that is, $q_x = 0.1, q_\phi = 0.05, q_{x\phi} = 1$, for cross-ply laminate configurations.

Design variables:

$$\xi = \{\xi_1^A, \xi_2^A, \xi_3^A, \xi_1^B, \xi_2^B, \xi_3^B, \xi_1^D, \xi_2^D, \xi_3^D\}^T$$

Subject to:

Eqs. (8), (9), (12), (13), (14), and (15)

For this constrained nonlinear optimization problem the feasible direction method combined with the golden section method is adopted. The optimization is carried out using the Automated Design Synthesis program¹⁷ for three cases in the design space of the nine lamination parameters:

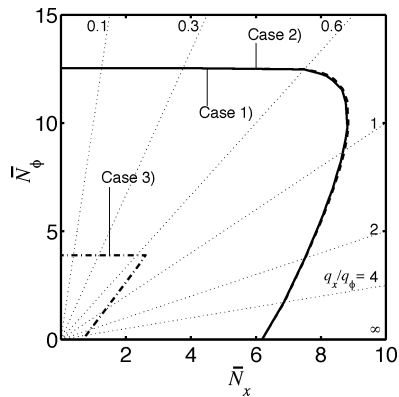
1) All nine of the lamination parameters, that is, $\xi_{1,2,3}^A, \xi_{1,2,3}^B$, and $\xi_{1,2,3}^D$, are used for optimization.

2) Three lamination parameters, that is, $\xi_1^{A,B,D}$, are used for optimization while $\xi_3^{A,D} = \xi_{2,3}^B = 0, \xi_2^{A,D} = 1$ are imposed.

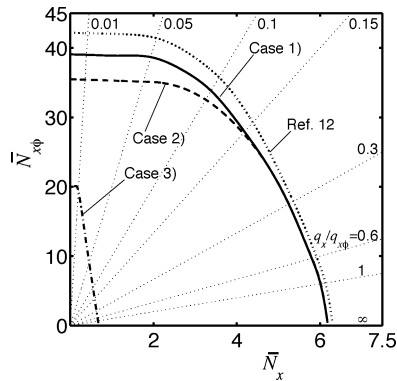
3) Three lamination parameters, that is, $\xi_3^{A,B,D}$, are used for optimization while $\xi_1^{A,D} = \xi_{1,2}^B = 0, \xi_2^{A,D} = -1$ are imposed.

Thus, in case 1 the layer angles of the laminated composite cylindrical shells are restricted to the values of 0, 45, -45 , and 90 deg, and in cases 2 and 3 cross-ply laminate configurations and angle-ply laminate configurations are considered, respectively.

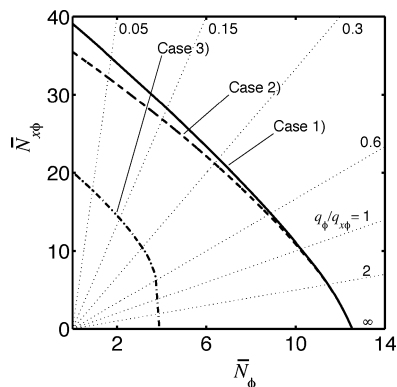
Figure 9 shows the comparisons of the highest normalized buckling loads \bar{N}_x , \bar{N}_ϕ , and $\bar{N}_{x\phi}$ for the three cases. The results are shown for loading ratios as combinations of axial compression and lateral pressure, axial compression and torsion, and lateral pressure and torsion corresponding to Figs. 9a–9c, respectively. For all of the loading ratios, case 3 shows the worst buckling loads. In Fig. 9a it can be observed that the best laminate configurations for the cylindrical shells subjected to combinations of axial compression and lateral pressure are cross-ply laminate configurations. The small difference between cases 1 and 2 is given by numerical inaccuracies. More accurate results are obtained using three design variables than using nine design variables. For combinations of axial compression and torsion, Fig. 9b shows that maximum \bar{N}_x is almost the same for cases 1 and 2. However, for loading ratios $q_x/q_{x\phi} \in [0, 0.15]$, case 1 gives better results. In Fig. 9b the maximum buckling loads obtained



a) Axial compression and lateral pressure, that is, $q_x/q_\phi \in [0, \infty)$, $q_{x\phi} = 0$



b) Axial compression and torsion, that is, $q_x/q_{x\phi} \in [0, \infty)$, $q_\phi = 0$



c) Lateral pressure and torsion, that is, $q_\phi/q_{x\phi} \in [0, \infty)$, $q_x = 0$

Fig. 9 Optimum buckling loads for combinations of axial compression, lateral pressure, and torsion.

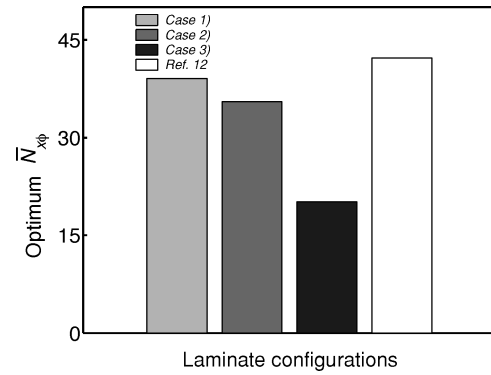


Fig. 10 Optimum $\bar{N}_{x\phi}$ in case of torsion, that is, $q_{x\phi} = 1$, $q_x = q_\phi = 0$.

in Ref. 12 for unrestricted laminate configurations are also shown by the dotted line. It can be seen that the difference between the buckling loads for case 1 and the buckling loads obtained in Ref. 12 increases when the torsional load increases. For combinations of lateral pressure and torsion, Fig. 9c shows that maximum \bar{N}_ϕ is almost the same for cases 1 and 2. For loading ratios $q_\phi/q_{x\phi} \in [0, 1)$, case 1 gives better results.

Figure 10 shows the maximum $\bar{N}_{x\phi}$ for laminated composites cylindrical shells subjected to torsion. By comparing the optimum buckling loads obtained in Ref. 12 with the optimum buckling loads obtained for cases 1, 2, and 3, we can observe differences of 7.4, 16, and 52.4%, respectively. Hence, it is inconsistent to restrict the layer angles of the laminated composite cylindrical shells only to cross-ply laminate configurations or to angle-ply laminate configurations. A difference of less than 10% for laminate configurations with layer angles restricted to the values of 0, 45, -45 , and 90 deg might be acceptable for practical use.

Optimum lamination parameters for maximizing the buckling loads for loading ratios were obtained on the boundary of the feasible region and are given in Table 3. Note that in the case of combination of axial compression and lateral pressure the optimum lamination parameters shows orthotropic characteristics, that is, $\xi_3^{A,B,D} = 0$. Moreover, these lamination parameters correspond to almost symmetric laminate configurations because $\xi_1^B = 0.02$ and $\xi_{2,3}^B = 0$. However, when the axial compression and the lateral pressure are combined with torsion, the optimum lamination parameters shows both nonorthotropic and nonsymmetric characteristics for the laminate configurations.

The laminate configurations aiming to realize the optimum lamination parameters are given in Table 4. For the cases of pure axial compression and pure lateral pressure, we obtained unidirectional laminates oriented at 0 and 90 deg, respectively. For all of the other cases we obtained laminate configurations with no physical meaning because the layer thicknesses are not integers. The cross-ply laminate configuration corresponding to the combination of axial compression and lateral pressure is calculated using the formulas given in Table 2. For the cases where the axial compression and the lateral pressure are combined with torsion, the laminate configurations are obtained with the proposed optimization procedure. For this optimization procedure, the Broyden–Fletcher–Goldfarb–Shanno (BFGS) method combined with golden section method was adopted in ADS program and a value $\varepsilon = 10^{-4}$ was used. This optimization procedure provides laminate configurations with no physical meaning, that is, the set of lamination parameters ξ calculated from these laminate configurations will match the optimum set of lamination parameters independent of the weighting functions $w_{1,2,3}^X$ ($X = A, B, D$). Thus, the weighting functions are set to be equal with one, that is, $w_{1,2,3}^X = 1$ ($X = A, B, D$). [In practice, when discrete optimization methods are employed for determining laminate configurations with integer layer thicknesses, the most near optimal laminate configuration is not necessary the best because the objective function of the layup optimization problem, that is, the critical loading parameter \bar{N} , has different sensitivities with respect to different lamination parameters. For selecting the best near-optimal

Table 3 Optimum lamination parameters for maximizing buckling loads

Loading ratio			Lamination parameter									Loading parameter \bar{N}
q_x	q_ϕ	$q_{x\phi}$	ξ_1^A	ξ_2^A	ξ_3^A	ξ_1^B	ξ_2^B	ξ_3^B	ξ_1^D	ξ_2^D	ξ_3^D	
1.00	0.00	0.00	1.00	1.00	0.00	0.00	0.00	0.00	1.00	1.00	0.00	6.189
0.00	1.00	0.00	-1.00	1.00	0.00	0.00	0.00	0.00	-1.00	1.00	0.00	12.540
0.00	0.00	1.00	-0.10	0.71	-0.14	0.02	-0.25	-0.13	-0.79	0.82	-0.09	39.083
1.00	0.50	0.00	0.81	1.00	0.00	0.02	0.00	0.00	0.47	1.00	0.00	8.407
0.10	0.00	1.00	0.36	0.80	-0.07	0.02	-0.19	-0.13	-0.34	0.74	-0.09	33.997
0.00	0.05	1.00	-0.19	0.76	-0.12	0.01	-0.19	-0.09	-0.85	0.88	-0.06	34.789
0.10	0.05	1.00	0.06	0.80	-0.06	0.03	-0.14	-0.11	-0.69	0.83	-0.06	33.504

Table 4 Laminate configurations for optimum lamination parameters

Loading ratio			Laminate configuration
q_x	q_ϕ	$q_{x\phi}$	
1.00	0.00	0.00	[0 _{1,00}]
0.00	1.00	0.00	[90 _{1,00}]
0.00	0.00	1.00	[90 _{0.274/0.377/-45_{0.143/90_{0.206}}}]
1.00	0.50	0.00	[90 _{0.052/0.903/90_{0.045}}]
0.10	0.00	1.00	[90 _{0.154/45_{0.015/0.611/-45_{0.087/0.017/90_{0.116}}}}]
0.00	0.05	1.00	[90 _{0.297/0.346/-45_{0.117/90_{0.240}}}]
0.10	0.05	1.00	[90 _{0.232/45_{0.018/0.478/-45_{0.083/90_{0.189}}}}]

laminate configuration from alternate possible designs, it might be appropriate to use the sensitivities of the objective function with respect to the optimum lamination parameters as weighting functions in Eq. (22), that is, $w_{1,2,3}^X = \partial \bar{N} / \partial \xi_{1,2,3}^X$ ($X = A, B, D$).] All of the laminate configurations correspond to optimum lamination parameters on the boundary of the feasible region since for every loading ratio the number of layers is less than seven.

Conclusions

The buckling loads of long laminated composite cylindrical shells with layer angles restricted to the values of 0, 45, -45, and 90 deg subjected to combinations of axial compression, external lateral pressure, and torsion were maximized using nine lamination parameters as design variables. The complete set of explicit expressions relating the nine lamination parameters was derived. Thus, using this set of explicit expressions, the layup optimization was carried out in a simple and efficient manner based on a mathematical programming method. The laminate configurations aiming to realize the optimum lamination parameters were also examined. For combinations of axial compression and lateral pressure, the optimum cross-ply laminate configurations can be calculated by analytic formulas. For the cases where the axial compression and the lateral pressure are combined with torsion, the optimum lamination parameters show nonorthotropic characteristics, and the optimum laminate configurations can be obtained using a mathematical programming method. A difference of less than 10% was obtained between the optimum for unrestricted laminate configurations compared with the optimum for laminate configurations with layer angles restricted to the values of 0, 45, -45, and 90 deg.

The set of explicit expressions describing the feasible region of the nine lamination parameters extends the use of lamination parameters to a large class of layup optimization problems involving mechanical couplings and/or combinations of in-plane and out-of-plane stiffnesses. Also, this set of explicit expressions makes the use of lamination parameters suitable and efficient for practical layup design in industry because the layer angles are restricted to the typical values of 0, 45, -45, and 90 deg used by manufacturers.

Appendix: Definition of Differential Operators H_{ij}

Denoting partial differentiation by a comma, the differential operators H_{ij} ($i, j = 1, 2, 3$) are defined as follows:

$$H_{11} = (A_{11} + B_{11})(\cdot)_{,xx} + 2(A_{16}/R)(\cdot)_{,x\phi} + (1/R^2)[A_{66} - B_{66}/R + D_{66}/R^2](\cdot)_{,\phi\phi} \quad (A1)$$

$$H_{12} = [A_{16} + 2(B_{16}/R) + D_{16}/R^2](\cdot)_{,xx} + (1/R)[A_{12} + A_{66} + (B_{12} + B_{66})/R](\cdot)_{,x\phi} + (A_{26}/R^2)(\cdot)_{,\phi\phi} \quad (A2)$$

$$H_{13} = -(B_{11} + D_{11}/R)(\cdot)_{,xxx} - (1/R)(3B_{16} + D_{16}/R)(\cdot)_{,xxx\phi} - (1/R^2)(B_{12} + 2B_{66} - D_{66}/R)(\cdot)_{,x\phi\phi} - (1/R^3)(B_{26} - D_{26}/R)(\cdot)_{,\phi\phi\phi} + (A_{12}/R)(\cdot)_{,x} + (1/R^2)(A_{26} - B_{26}/R + D_{26}/R^2)(\cdot)_{,\phi} \quad (A3)$$

$$H_{22} = [A_{66} + 3(B_{66}/R) + 3(D_{66}/R^2)](\cdot)_{,xx} + (2/R)[A_{26} + 2(B_{26}/R) + D_{26}/R^2](\cdot)_{,x\phi} + (1/R)(A_{22} + B_{22}/R)(\cdot)_{,\phi\phi} \quad (A4)$$

$$H_{23} = -[B_{16} + 2(D_{16}/R)](\cdot)_{,xxx} - (1/R)[B_{12} + 2B_{66} + (D_{12} + 3D_{66})/R](\cdot)_{,xxx\phi} - (1/R^2)[3B_{26} + 2(D_{26}/R)](\cdot)_{,x\phi\phi} - (B_{22}/R^3)(\cdot)_{,\phi\phi\phi} + (1/R)(A_{26} + B_{26}/R)(\cdot)_{,x} + (A_{22}/R^2)(\cdot)_{,\phi} \quad (A5)$$

$$H_{33} = D_{11}(\cdot)_{,xxx} + 4(D_{16}/R)(\cdot)_{,xxx\phi} + (2/R^2)(D_{12} + 2D_{66})(\cdot)_{,xx\phi\phi} + 4(D_{26}/R^3)(\cdot)_{,x\phi\phi\phi} + (D_{22}/R^4)(\cdot)_{,\phi\phi\phi\phi} + 2(B_{12}/R)(\cdot)_{,xx} + (2/R^2)(2B_{26} - D_{26}/R)(\cdot)_{,x\phi} + (2/R^3)(B_{22} - D_{22}/R)(\cdot)_{,\phi\phi} + (1/R)(A_{22} - B_{22}/R + D_{22}/R^2) \quad (A6)$$

where the terms A_{ij} , B_{ij} , and D_{ij} ($i, j = 1, 2, 6$) are the in-plane, the coupling, and the out-of-plane stiffnesses, respectively.

References

- Nshanian, Y. S., and Pappas, M., "Optimal Laminated Composite Shells for Buckling and Vibration," *AIAA Journal*, Vol. 21, No. 3, 1983, pp. 430-437.
- Sun, G., and Hansen, J. S., "Optimal Design of Laminated Composite Circular-Cylindrical Shells Subjected to Combined Loads," *Journal of Applied Mechanics*, Vol. 55, No. 1, 1988, pp. 136-142.
- Zimmermann, R., "Quick Optimum Buckling Design of Axially Compressed, Fiber Composite Cylindrical Shells," *AIAA Journal*, Vol. 33, No. 10, 1995, pp. 1993-1995.
- Riche, R. L., and Haftka, R. T., "Optimization of Laminate Stacking Sequence for Buckling Load Maximization by Genetic Algorithm," *AIAA Journal*, Vol. 31, No. 5, 1993, pp. 951-956.

⁵Nagendra, S., Jestin, D., Gürdal, Z., Haftka, R. T., and Watson, L. T., "Improved Genetic Algorithm for the Design of Stiffened Composite Panels," *Computers and Structures*, Vol. 58, No. 3, 1996, pp. 543–555.

⁶McMahon, M. T., Watson, L. T., Soremekun, G. A., Gürdal, Z., and Haftka, R. T., "A Fortran 90 Genetic Algorithm Module for Composite Laminated Structure Design," *Engineering with Computers*, Vol. 14, No. 3, 1998, pp. 260–273.

⁷Onoda, J., "Optimal Laminated Configurations of Cylindrical Shells for Axial Buckling," *AIAA Journal*, Vol. 23, No. 7, 1985, pp. 1093–1098.

⁸Grenestedt, J. L., and Gudmundson, P., "Layup Optimization of Composite Material Structures," *Proceedings of IUTAM Symposium on Optimal Design with Advanced Materials*, edited by P. Petersen, Elsevier Science, Amsterdam, 1993, pp. 311–336.

⁹Fukunaga, H., and Vanderplaats, G. N., "Stiffness Optimization of Orthotropic Laminated Composites Using Lamination Parameters," *AIAA Journal*, Vol. 29, No. 4, 1991, pp. 641–646.

¹⁰Diaconu, C. G., Sato, M., and Sekine, H., "Feasible Region in General Design Space of Lamination Parameters for Laminated Composites," *AIAA Journal*, Vol. 40, No. 3, 2002, pp. 559–565.

¹¹Diaconu, C. G., Sato, M., and Sekine, H., "Layup Optimization of Symmetrically Laminated Thick Plates for Fundamental Frequencies Using Lam-

ination Parameters," *Structural and Multidisciplinary Optimization*, Vol. 24, No. 4, 2002, pp. 302–311.

¹²Diaconu, C. G., Sato, M., and Sekine, H., "Buckling Characteristics and Layup Optimization of Long Laminated Composite Cylindrical Shells Subjected to Combined Loads Using Lamination Parameters," *Composite Structures*, Vol. 58, No. 4, 2002, pp. 423–433.

¹³Cheng, S., and Ho, B. P. C., "Stability of Heterogeneous Aeolotropic Cylindrical Shells Under Combined Loads," *AIAA Journal*, Vol. 1, No. 4, 1963, pp. 892–898.

¹⁴Whitney, J. M., and Sun, C. T., "Buckling of Composite Cylindrical Characterization Specimens," *Journal of Composite Materials*, Vol. 9, No. 4, 1975, pp. 138–148.

¹⁵Tsai, S. W., and Hahn, H., *Introduction to Composite Materials*, Technomic, Lancaster, PA, 1980, pp. 232–239.

¹⁶Gürdal, Z., Haftka, R. T., and Hajela, P., *Design and Optimization of Laminated Composite Materials*, 1st ed., Wiley, New York, 1999, Chap. 4.

¹⁷Vanderplaats, G. N., and Sugimoto, H., "A General-Purpose Optimization Program for Engineering Design," *Computers and Structures*, Vol. 24, No. 1, 1986, pp. 13–21.

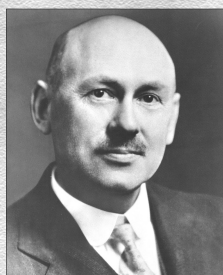
B. Sankar
Associate Editor



R O C K E T S



The two most significant publications in the history of rockets and jet propulsion are *A Method of Reaching Extreme Altitudes*, published in 1919, and *Liquid-Propellant Rocket Development*, published in 1936. All modern jet propulsion and rocket engineering are based upon these two famous reports.



Robert H. Goddard

It is a tribute to the fundamental nature of Dr. Goddard's work that these reports, though more than half a century old, are filled with data of vital importance to all jet propulsion and rocket engineers. They form one of the most important technical contributions of our time.

By arrangement with the estate of Dr. Robert H. Goddard and the Smithsonian Institution, the American Rocket Society republished the papers in 1946. The book contained a foreword written by Dr. Goddard just four months prior to his death on 10 August 1945. The book has been out of print for decades. The American Institute of Aeronautics and Astronautics is pleased to bring this significant book back into circulation.

2002, 128 pages, Paperback
ISBN: 1-56347-531-6
List Price: \$31.95
AIAA Member Price: \$19.95

Order 24 hours a day at www.aiaa.org
Publications Customer Service, P.O. Box 960, Herndon, VA 20172-0960
Fax: 703/661-1501 • Phone: 800/682-2422 • E-mail: warehouse@aiaa.org